



## Article

# The Behaviour of Rare Earth Elements from South African Coal Fly Ash during Enrichment Processes: Wet, Magnetic Separation and Zeolitisation

Mero-Lee Ursula Cornelius <sup>1,\*</sup>, Alechine Emmanuel Ameh <sup>1</sup>, Chuks Paul Eze <sup>1</sup>, Olanrewaju Fatoba <sup>1</sup>, Asel Sartbaeva <sup>2</sup> and Leslie Felicia Petrik <sup>1</sup>

<sup>1</sup> Department of Chemistry, University of the Western Cape, Bellville, Cape Town 7535, South Africa; eameh@uwc.ac.za (A.E.A.); ceze@uwc.ac.za (C.P.E.); ofatoba@uwc.ac.za (O.F.); lpetrik@uwc.ac.za (L.F.P.)  
<sup>2</sup> Department of Chemistry, University of Bath, Bath BA2 7AY, UK; as2413@bath.ac.uk  
\* Correspondence: meroleecornelius@gmail.com

**Abstract:** Rare earth elements (REEs) are essential raw materials in a variety of industries including clean energy technologies such as electric vehicles and wind turbines. This places an ever-increasing demand on global rare earth element production. Coal fly ash (CFA) possesses appreciable levels of REEs. CFA, a waste by-product of coal combustion, is therefore a readily available source of REEs that does not require mining. CFA valorisation to zeolites has been achieved via various synthesis pathways. This study aimed to evaluate one such pathway by monitoring how REEs partition during CFA processing by the wet, magnetic separation process and zeolitisation. South African CFA was subjected to wet, magnetic separation and subsequent zeolitisation of the nonmagnetic fraction (NMF); solid products were characterised by XRD, SEM, XRF and LA-ICP-MS. The wet, magnetic separation process resulted in the partitioning of a specific set of transition metals (such as Fe, Mn, Cr, V, Ni, Zn, Cu, Co and Mo) into the magnetic fraction (MF) of CFA, while REEs partitioned into the NMF with a total REE content of 530.2 ppm; thus, the matrix elements of CFA were extracted with ease. Zeolitisation resulted in a solid zeolite product (hydroxysodalite) with a total REE content of 537.6 ppm. The process of zeolitisation also resulted in the selective enrichment of Ce (259.1 ppm) into the solid zeolite product (hydroxysodalite), while other REEs were largely partitioned into the liquid phase. CFA valorisation by wet, magnetic separation and zeolitisation therefore allowed for the partitioning of REEs into various extraction products while recovering the matrix elements of CFA such as Fe, Si and Al. The findings of this study highlight the geopolitical importance of REEs in terms of the development of alternative processes for REE recovery from waste and alternative sources, which may potentially give countries that employ and develop the technology a key advantage in the production of REEs for the global market.

**Keywords:** coal fly ash; coal combustion products; rare earth elements; magnetic separation; zeolitisation



**Citation:** Cornelius, M.-L.U.; Ameh, A.E.; Eze, C.P.; Fatoba, O.; Sartbaeva, A.; Petrik, L.F. The Behaviour of Rare Earth Elements from South African Coal Fly Ash during Enrichment Processes: Wet, Magnetic Separation and Zeolitisation. *Minerals* **2021**, *11*, 950. <https://doi.org/10.3390/min11090950>

Academic Editor: Kenneth N. Han

Received: 7 July 2021

Accepted: 11 August 2021

Published: 31 August 2021

**Publisher's Note:** MDPI stays neutral with regard to jurisdictional claims in published maps and institutional affiliations.



**Copyright:** © 2021 by the authors. Licensee MDPI, Basel, Switzerland. This article is an open access article distributed under the terms and conditions of the Creative Commons Attribution (CC BY) license (<https://creativecommons.org/licenses/by/4.0/>).

## 1. Introduction

Rare earth elements (REEs) are a group of 17 elements including the lanthanide series (15 elements) as well as yttrium and scandium [1]. REEs have very good catalytic, electronic, magnetic and optical properties. As such, in the last few decades REEs have attracted great interest from many sectors namely the motor, petroleum and medical industry, as well as clean energy applications (such as electric vehicle and wind turbine production) [1,2]. The increasing need for REEs, particularly for clean energy applications, creates a higher demand for REE production globally. REE deposits are found in naturally occurring minerals in the earth's (upper) crust at a total abundance of 183.1 ppm [3,4]. The abundance of REEs in the earth's crust ranges from 63 ppm for Ce (the most abundant REE) to 0.30 ppm for Tm (the least abundant REE) [4,5].

Native elemental REE metals are not found in nature. However, REEs have been found in more than 200 minerals (mainly in igneous rocks) [2,6]. Four main mineral sources are currently utilised for REE production; bastnäsite (China), monazite (Australia and India), xenotime (Malaysia) and loparite (Russia) [2]. The recovery of REEs from these minerals typically involves mining and extensive processing that incorporates chemical and/or physical methods (such as roasting, alkaline or acidic leaching, etc.) to break down the matrix minerals in which REEs are found [7–9]. Considering the complex steps involved in REE recovery as well as the relatively low concentration of REEs in the earth's crust, the cost-effective extraction and recovery of REEs from natural deposits is still beyond our reach [1].

In recent years, coal and coal combustion by-products have attracted attention due to the potential for these naturally occurring and waste materials to serve as alternative sources for REE recovery [10–13]. Coal is known to naturally contain relatively high levels of REEs compared to the Earth's upper crust. Coal and coal fly ash (CFA) are composed of varying levels of REE-containing minerals bastnäsite, monazite as well as xenotime, depending on the location of the deposit [9,14]. CFA is a waste by-product of coal combustion that is produced in millions of tons globally, in countries such as South Africa, USA, China, India, Australia, Greece, Japan and Poland [12,15]. Large scale CFA disposal is associated with negative environmental impacts such as soil and water pollution that has detrimental effects on agriculture and aquatic life [16–18]. As such, the valorisation of CFA has been the focus of much research over the years. The utilisation of CFA in the building and construction industry has been extensively explored for the production of concrete and building materials as a relatively less expensive feedstock [19,20], as well as in the production of geo-polymers [15,21,22]. Other applications include CFA utilisation for mine back-filling, as well as agricultural remediation of soil and water treatment using modified CFA [17,23]. Another major area of research in CFA valorisation is the production of value-added, porous materials such as zeolites (i.e., zeolitisation) as well as metal extraction/recovery [24–35]. As South Africa is largely reliant on coal for energy production [15], CFA research and the development of various CFA valorisation technologies remain major priorities.

South African CFA from the Matla power station in Mpumalanga was previously reported as a potential source of REEs, with a total abundance of ~480 ppm [17]. In another study, a set of six CFA samples (three from Poland and three from the United Kingdom) were also reported to contain appreciable REE levels between 246 and 481 ppm [36]. Various pre-processing technologies, such as flotation, separation by gravitational force and magnetic (dry or wet) separation, are commonly employed to enrich REEs in natural minerals [7,37]. Similarly, CFA has been processed by physical separation methods such as size classification and magnetic separation [27,38,39], in some cases, for the purpose of REE enrichment [14,36,40,41]. Table 1 summarises the REE enrichment factors of CFA samples treated by either magnetic separation (dry), size classification or a combination of both pre-processing steps, as reported in literature. Lin et al. [14] reported that dry magnetic separation resulted in the enrichment of REEs into the nonmagnetic fraction (NMF) material for a range of different CFA samples from the United States of America, and that REE enrichment factors between 1.01 and 1.13 were observed depending on the CFA feedstock. The processing of CFA by size classification resulted in the partitioning of REEs mainly into the smallest fraction of CFA, with mean particle size < 2.2 µm (enrichment factor of 1.33), while an enrichment factor of 1.08 was reported for REEs in the relatively larger size fraction of CFA (mean particle size < 19.4 µm) [40]. In another study, a combination of pre-processing methods including size classification and dry, magnetic separation resulted in REE enrichment into the smallest fraction < 38 µm of CFA (UK) by a factor of 1.18 [36]. It is noteworthy that these pre-processing methods resulted in only minor enrichment of REEs.

**Table 1.** REE enrichment factors in CFA by various physical pre-processing methods reported in literature.

REE	Size Classification (<2.2 µm)	Size Classification (<19.4 µm)	Size Classification and Magnetic Separation
	Lanzerstorfer, [40]		Blissett et al. [36]
La	1.19	1.35	1.06
Ce	1.09	1.21	1.01
Pr	1.30	1.20	1.12
Nd	1.05	1.19	1.07
Sm	1.15	1.23	1.10
Eu	1.23	1.03	1.25
Gd	1.21	1.00	1.31
Tb	1.36	1.05	1.21
Dy	1.20	1.00	1.36
Ho	1.34	0.97	1.23
Er	1.45	0.96	1.30
Tm	1.55	1.00	1.22
Yb	1.65	0.99	1.19
Lu	1.62	1.00	1.13
EF (REEs)	1.31	1.08	1.18

A recent review proposed a multi-stage process may be an efficient pathway for recovery of REEs from CFA [5]. Lin et al. [42] reported a seven-step sequential extraction process involving dissolution, ion-exchange and various leaching steps was evaluated as a potential route for REE enrichment from CFA. Lin et al. [42] also evaluated physical separation methods, including size classification and magnetic separation, as well as alkaline, hydrothermal treatment for REE enrichment from CFA. It was reported that the glassy, aluminosilicate phase of CFA contained the majority of the REE content and a process involving size classification, magnetic separation and hydrothermal treatment was proposed as a method of enriching the REE content of CFA [42]. Zeolitisation is a common method utilised in the transformation of the Si and Al content in CFA into a crystalline, porous material with high industrial value [24–26,28–34]. The distributional fate of elements found in CFA during the process of zeolitisation by two different methods (a two-step process and solid fusion-assisted process) was previously reported in literature [26]. Du Plessis et al. [26] emphasised the fate of toxic elements such as Al, As, Hg, Nb and Pb during the transformation of CFA to zeolite A and P; it was reported that these elements were mainly present in the supernatant solution (and washing solution) after zeolitisation. REEs Ce and Y were reported to be recovered in the bulk solid products of the two different methods. During the two-step process, Ce and Y were 100 wt% retained in the zeolite product (Na-P1 and Analcime). On the other hand, 100 wt% of Ce and Y was found in the solid waste product during the solid fusion process for zeolite A formation. However, the fate of all the other REEs found in South African CFA during processing by zeolitisation was not monitored.

CFA conversion to zeolites has become a favourable route for valorisation of this waste by-product to an industrially valuable material, which may be coupled to the recovery of other matrix elements such as Al, Fe and Si depending on the type of processing applied [27,34]. CFA processing by wet, magnetic separation prior to zeolitisation, and coupled to Si recovery from the supernatant solution, has become a favourable route for zeolite production due to the ability to recover the matrix elements of CFA such as Fe, Si and Al for further utilisation in various applications [27,34]. Therefore, in this study, CFA will be processed by wet, magnetic separation and subsequent zeolitisation, coupled to Si extraction from the zeolitisation supernatant via precipitation. Under these CFA valorisation conditions, the matrix elements of CFA such as Fe and Si may be recovered as solid products while the bulk of CFA is converted to a crystalline zeolite. Due to the geopolitical importance of REEs and the great demand for REE production and supply to the global market, this study aimed to monitor how REEs partition between these different

fractions of CFA (nonmagnetic and magnetic) and zeolitisation products (hydroxysodalite and Si extract) during processing.

## 2. Experimental Methods

CFA was sourced from the Arnot power station in Mpumalanga, South Africa and processed by wet, magnetic separation followed by zeolitisation, as illustrated in Figure 1.

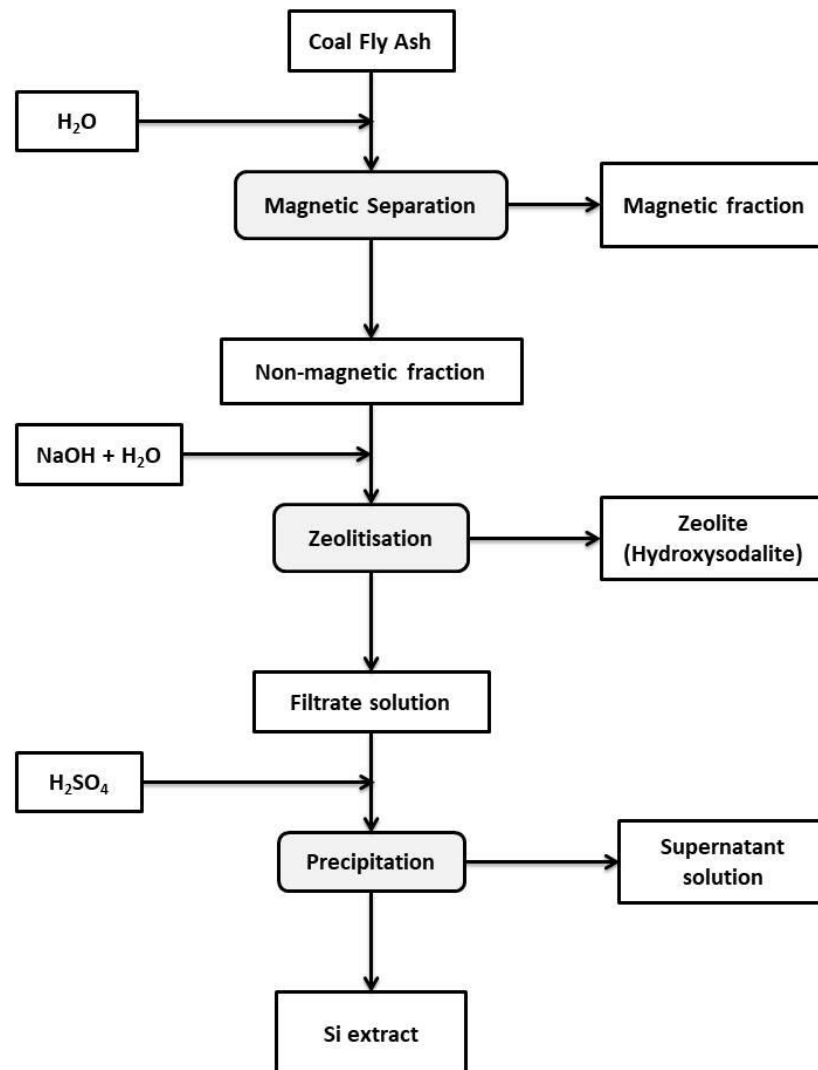


**Figure 1.** The overview of CFA processing by wet, magnetic separation and zeolitisation as well as Si recovery via precipitation.

### 2.1. Magnetic Separation Process

As-received South African CFA was subjected to magnetic separation of the iron-containing mineral phases present in CFA by applying similar conditions to those reported in the literature using small scale, basic laboratory equipment [27,43]. South African CFA was mixed with deionised water at a solid to liquid ratio of 1:2 and stirred for 6 h. A magnet was used to separate the magnetic fraction (MF) of CFA, and the NMF of CFA was collected by filtration. The solid products were dried overnight in an oven at 90 °C and characterised by X-ray diffraction (XRD), Scanning electron microscopy (SEM), X-ray fluorescence spectroscopy (XRF) and Laser ablation-inductively-coupled plasma-mass spectrometry (LA-ICP-MS).

## 2.2. Zeolitisation of Nonmagnetic Fraction and Si Recovery

The NMF was mixed with an 8.0 M NaOH solution at a set ratio and subjected to stirred, alkaline reflux conditions of 150 °C for 24 h. The zeolitisation conditions were chosen based on the optimal dissolution of silicate species into the filtrate solution, as reported in literature [34], and concurrent conversion of the nonmagnetic fraction of CFA to a solid zeolite product. The solid product was collected by filtration and dried in an oven overnight at 70 °C. The filtrate was collected and conc. H<sub>2</sub>SO<sub>4</sub> was added drop-wise to initiate Si precipitation. The Si extract was then collected by filtration and dried in an oven overnight at 70 °C.

## 2.3. Characterisation

The mineralogical and elemental (major and trace) composition of solid products of the magnetic separation (namely, the magnetic fraction and nonmagnetic fraction) and zeolitisation process (namely, the zeolite and Si extract) were determined by XRD, XRF and LA-ICP-MS, respectively. XRD analysis was carried out on a powder Bruker D8-Advance X-ray diffractometer (iThemba Labs, Cape Town, South Africa) measurements were carried out at 40 kV and 25 mA with Cu K $\alpha$ <sub>1</sub> radiation ( $\lambda = 0.154$  nm). The morphological properties of the magnetic separation products were analysed by SEM. SEM analysis of powdered solid products was carried out on a Zeiss Auriga field emission gun (FEG)-scanning emission microscope at 5.0 kV (Department of Physics, University of the Western Cape, Cape Town, South Africa). XRF analysis of solid products was carried out on a PANalytical Axios Wavelength Dispersive spectrometer fitted with a Rh tube and scintillation detector, using SuperQ PANalytical software (CAF unit, University of Stellenbosch, Stellenbosch, South Africa). XRF conditions were set at 50 kV and 50 mA. LA-ICP-MS analysis was carried out on an Agilent 7500ce ICP-MS spectrometer, fitted with a Resonetics 193 nm Excimer laser (CAF unit, University of Stellenbosch, Stellenbosch, South Africa). Elemental analyses were all carried out in triplicate to determine the relative standard deviation and the weight percentage of a particular element/oxide (wt%) was calculated according to Equation (1). The enrichment of the various elements of CFA into the different process products (MF, NMF, zeolite and Si extract) was calculated according to Equation (2) adapted from literature [14]; the enrichment factor (EF) for a particular element was calculated relative to the quantity of that element in CFA.

$$\begin{aligned} \text{Weight percentage of } x \text{ (wt\%}_x\text{)} \\ = \text{Average Dry Mass}_x / \text{Total Dry Mass}_{\text{CFA}} \times 100 \end{aligned} \quad (1)$$

$$\text{Enrichment factor (EF)} = \text{Quantity}_x / \text{Quantity}_{x\text{CFA}} \quad (2)$$

## 3. Results and Discussion

### 3.1. Characterisation of Coal Fly Ash

#### 3.1.1. Mineralogical and Morphological Analysis of Coal Fly Ash

The mineralogical content and morphology of as-received CFA was determined by XRD and SEM, respectively (depicted in Figure 2). The main mineral phases present in CFA were quartz (SiO<sub>2</sub>) and mullite (3Al<sub>2</sub>O<sub>3</sub>2SiO<sub>2</sub>), which are composed of silicate and aluminosilicate minerals, respectively. Diffraction peaks corresponding to magnetite (Fe<sub>3</sub>O<sub>4</sub>) were present in CFA; this mineral phase is composed of iron (II/III) oxides. CFA is also known to contain other iron oxide mineral phases such as hematite ( $\alpha$ -Fe<sub>2</sub>O<sub>3</sub>) [44,45]. Both iron oxide mineral phases are magnetic; magnetite is ferromagnetic with relatively high magnetism (92 Am<sup>2</sup>/kg) compared to hematite, which is considered a canted antiferromagnetic mineral phase with a relatively weaker magnetism (0.4 Am<sup>2</sup>/kg) [46]. On the other hand, silicon-rich minerals such as quartz are known to be diamagnetic [47]. Therefore, the magnetic separation of iron oxide based mineral phases from the other matrix elements of CFA such as Si and Al was possible.

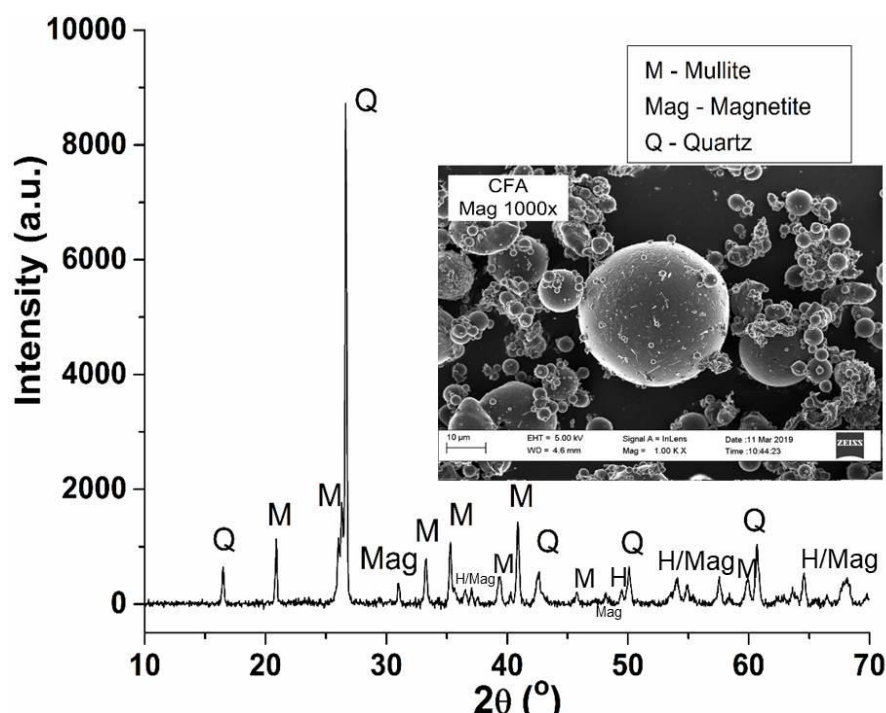


**Figure 2.** Powder XRD pattern of as-received coal fly ash (CFA) with SEM micrograph (1000 $\times$ ) as an inset.

The presence of large particles ( $\sim 60$ – $175 \mu\text{m}$ ) with an irregular shape and relatively smaller, spherical particles ( $0.5$ – $40 \mu\text{m}$ ) were observed in as-received CFA (as depicted in Figure 2). The smooth appearance of these spherical CFA particles is attributed to aluminosilicate (glass-like) coatings that were formed during the high temperature coal combustion process. CFA morphology is significantly influenced by the thermal processing of coal and as such, the combustion temperature applied to coal as well as the post-combustion cooling (rate) plays a role in the nature and morphology of the resultant CFA [16,48]. The presence of rod-like particles on the surface of the spherical CFA particles is attributed to iron oxide mineral phases such as magnetite and hematite adhered to the surface of the glassy phase in CFA [49].

### 3.1.2. Chemical Composition of Coal Fly Ash

The chemical composition of as-received CFA was analysed by XRF (major oxide composition) and LA-ICP-MS (trace elemental composition), as listed in Tables 2 and 3, respectively. As listed in Table 2, CFA was classified as class F type fly ash due to the high total content of Si, Al and Fe oxides ( $>70 \text{ wt}\%$ ) [11]. Soluble elements such as Na and K typically occur in association with silicate and aluminosilicate based mineral phases in coal. Other elemental oxides (Ca, Cr, Mg, Mn, P, K, Na and Ti) were also present in major and minor quantities in as-received CFA. These elements are known to occur in the common mineral phases found in coal for example Apatite (Ca, P), Calcite (Ca), Dolomite (Ca, Mg), Gypsum (Ca), Chromite (Cr, Mg), Ankerite (Ca, Mg, Mn), Anatase (Ti) and Rutile (Ti) [50]. CFA exhibited a high L.O.I. value of  $\sim 7.7 \text{ wt}\%$ , which corresponds to the unburnt carbon content present in CFA. It should be noted that moisture in the CFA material may also contribute to the L.O.I value observed [15,16,51].

CFA contained a variety of elements in trace quantities, as listed in Table 2, i.e., elements that are useful nutrients for plants such as Cu and Zn as well as elements that may be harmful to animal and plant life such as Ni, Pb, Sr and Zr [26,52]. Furthermore, 16 out of 17 of the REEs (marked with \* in Table 3) were present in CFA in relatively high quantities compared to the REE abundance in the earth's upper crust. The most abundant REE in the earth's upper crust is Ce (63 ppm), typically mined from naturally occurring

mineral ore resources such as monazite and bastnäsite. Comparatively, CFA is almost 3 times more abundant in Ce (174 ppm) than natural resources in the earth's crust [4,53,54]. The total REE abundance in CFA was 490.5 ppm, i.e., more than twice the abundance of REEs in the earth's upper crust (183.1 ppm) [1,4,5].

**Table 2.** Major oxide composition (dry weight) of as-received CFA characterised by XRF spectroscopy (n = 3). L.O.I.: Loss on ignition; -: not applicable.

Major Elements	wt%	Relative Standard Deviation
SiO <sub>2</sub>	56.42	0.28
Al <sub>2</sub> O <sub>3</sub>	27.63	0.29
Fe <sub>2</sub> O <sub>3</sub>	6.08	1.24
CaO	5.62	0.45
TiO <sub>2</sub>	1.59	0.55
MgO	1.57	0.29
K <sub>2</sub> O	0.57	1.21
P <sub>2</sub> O <sub>5</sub>	0.36	2.04
Na <sub>2</sub> O	0.09	4.66
MnO	0.05	8.05
Cr <sub>2</sub> O <sub>3</sub>	0.02	0.12
Sum	100.00	-
L.O.I.	7.66	1.57

**Table 3.** Trace elemental composition of as-received CFA characterised by LA-ICP-MS spectroscopy (n = 3). \*: Rare earth element.

Trace Elements	Concentration (ppm)	Relative Standard Deviation
Ba	886.33	0.14
Sr	806.20	0.43
Zr	418.67	1.53
Ce *	174.30	0.14
V	125.67	0.70
La *	85.60	0.66
Ni	67.27	4.11
Y *	65.37	0.59
Nd *	65.23	1.16
Zn	50.80	1.32
Pb	39.82	0.14
Cu	38.20	0.77
Th	32.30	0.27
Nb	30.26	0.66
Rb	27.54	1.17
Sc *	26.27	0.51
Co	24.37	1.63
Pr *	18.38	0.80
Sm *	12.74	0.74
Gd *	11.38	0.76
Dy *	11.27	1.51
Hf	10.72	0.36
U	8.64	0.38
Er *	6.30	2.34
Yb *	5.76	0.65
Cs	4.93	2.57
Mo	4.56	7.04
Eu *	2.29	3.63
Ta	2.26	5.11
Ho *	2.21	1.24
Tb *	1.72	4.28
Tm *	0.87	2.04
Lu *	0.81	1.95

Waste electrical and electronic equipment (WEEE) such as mobile phones, polished LCD screens and computer hardware have also been evaluated as a potential resource for REE recovery. WEEEs typically contain Ce content of up to ~66 ppm, this value varies depending on the application [55–57] and is comparable to the REE abundance in the earth's upper crust. However, REE content in WEEEs is almost three times less than the REE abundance in CFA. South African CFA from the Arnot power station therefore contained enriched REE levels (490.5 ppm) compared to most other REE sources (natural and waste) as well as most fly ash samples from Poland (308–359 ppm) and USA (246–481 ppm) [36]. High REE levels were also reported for CFA from the Matla power station in South Africa [17]. The recovery of REEs from this readily available waste material (CFA) may therefore serve as a cheaper, enriched alternative to natural sources such as bastnäsite, monazite, xenotime as well as loparite, which all require mining. However, it should be noted that these REEs are present in CFA in close association with matrix elements such as Si, Al and Fe found in the main crystalline minerals of CFA. CFA also contains potentially radioactive elements Th and U in trace amounts. However, this drawback also exists for the extraction and recovery of REEs from natural resources [1,2].

### 3.2. Magnetic Separation

#### 3.2.1. Mineralogical Composition of the Magnetic and Nonmagnetic Fraction of CFA

Wet, magnetic separation of the iron-containing mineral phases in CFA was carried out in this study, resulting in the magnetic separation products (MF and NMF). The variation in the mineralogical content between CFA, MF and NMF was analysed by XRD (depicted in Figure 3). The diffraction pattern of the NMF material was similar to that of CFA, containing mainly quartz and mullite as well as minor magnetite diffraction peaks. The presence of Fe oxide mineral phases (magnetite and hematite) was observed in the MF material, together with quartz and minor mullite diffraction peaks [44,45,58]. During the magnetic separation process, most of the Fe-containing mineral phases were removed from the bulk of the CFA to yield the NMF material. However, the presence of Si-containing minerals was observed in the MF material due to the adherence of magnetic particles to glassy phase particles in CFA (see Figure S1, Supplementary Information).

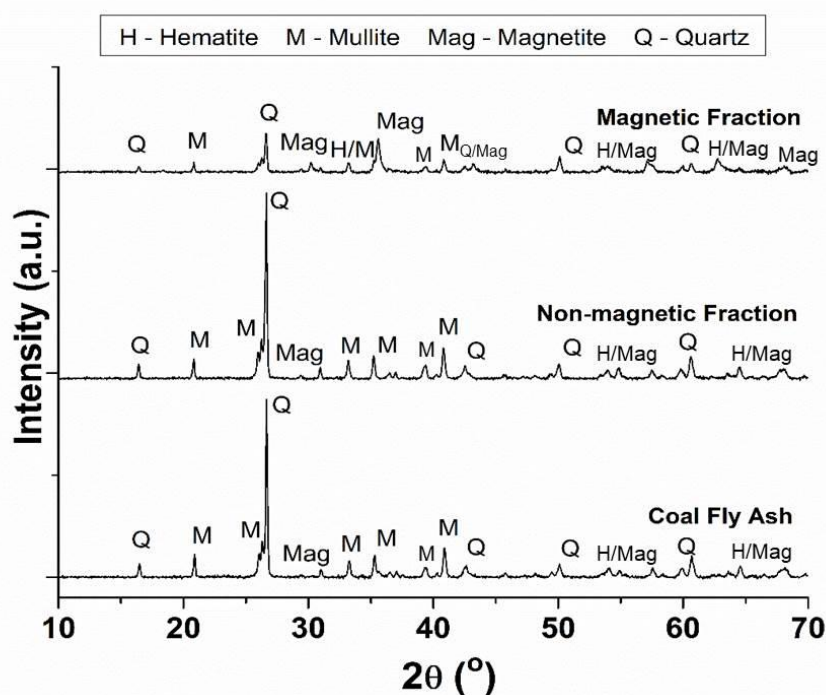


**Figure 3.** Powder XRD patterns of as-received CFA, magnetic fraction (MF) and nonmagnetic fraction (NMF) generated by wet magnetic separation.



### 3.2.2. Chemical Composition of the Magnetic and Nonmagnetic Fraction of CFA

The elemental composition of MF and NMF was analysed by XRF and LA-ICP-MS as listed in Tables 4 and 5, respectively. The NMF material contained a similar composition (in terms of major elements) as as-received CFA with SiO<sub>2</sub> and Al<sub>2</sub>O<sub>3</sub> content >70 wt% (as listed in Table 4). On the other hand, the MF material was composed of mainly Fe oxides (45.6 wt%), as well as Si (31.1 wt%) and Al (14.9 wt%) oxides. The chemical composition of CFA and the magnetic separation products (NMF and MF) corresponds well with the mineralogical analysis of these products (presented in Figure 3), with the separation of Fe oxides into the MF material accompanied by the partitioning of Si and Al oxides into the NMF material. Furthermore, the NMF material was mainly free of Fe oxides, while the MF material contained some Si and Al oxides. In terms of trace elemental composition, the NMF material was comparable to that of CFA (as listed in Table 4). On the other hand, a clear variation was observed in the trace elemental composition of the MF material compared to CFA, particularly for transition metal elements V, Ni, Zn, Cu, Co and Mo.

**Table 4.** Major oxide composition (dry weight) of the fractions of CFA (NMF and MF) characterised by XRF spectroscopy (n = 3), as well as the enrichment factor (EF) of each component relative to CFA. -: not applicable.

Major Elements	Nonmagnetic Fraction			Magnetic Fraction		
	wt%	Relative Standard Deviation	EF	wt%	Relative Standard Deviation	EF
SiO <sub>2</sub>	57.88	0.31	1.03	31.06	2.32	0.55
Al <sub>2</sub> O <sub>3</sub>	29.86	0.36	1.08	14.88	1.02	0.54
Fe <sub>2</sub> O <sub>3</sub>	2.70	0.09	0.44	45.57	3.69	7.49
CaO	5.24	0.12	0.93	4.84	0.12	0.86
TiO <sub>2</sub>	1.66	0.01	1.04	0.94	0.06	0.59
MgO	1.52	0.02	0.97	1.89	0.02	1.20
K <sub>2</sub> O	0.61	0.00	1.06	0.28	0.02	0.48
P <sub>2</sub> O <sub>5</sub>	0.37	0.00	1.03	0.29	0.01	0.81
Na <sub>2</sub> O	0.09	0.01	0.97	0.03	0.01	0.36
MnO	0.04	0.00	0.82	0.19	0.01	3.59
Cr <sub>2</sub> O <sub>3</sub>	0.02	0.00	1.01	0.02	0.00	1.18
Sum	100.00	-	-	100.00	-	-
L.O.I	8.03	0.20	-	0.40	0.28	-

#### Enrichment of Major Elements of CFA Components by Wet Magnetic Separation

The enrichment factors of the major oxides in the MF and NMF material are listed in Table 4. Compared to CFA, the MF material contained enriched levels of Fe, Mn, Cr as well as Mg oxides (EF values > 1). A high enrichment of Fe and Mn oxides was achieved in the MF material with EF values of ~7.5 and ~3.6, respectively, by using the magnetic separation process. Fe and Mn oxides present in CFA are known to be associated in mineral form [39,51,59], for example, in mineral phases such as ankerite, columbite and messelite [50]. Ferro-manganese oxides present as coatings in CFA were also reported by Ibrahim, [51]. Similarly, CFA leaching studies under varying conditions (such as pH) reported that Fe and Mn were present in close association on the surface of silicate particles in CFA [59]. Due to the complex nature of CFA, the recoveries of Fe and Mn in the MF material were relatively low, i.e., 64 and ~30 wt%, respectively (Table S1, Supplementary Information). The recovery of Fe into the MF and enrichment of REEs into the NMF may be further improved by repeated magnetic separation and/or utilisation of a stronger magnet in the separation process as reported in literature [27,43].

The NMF material contained slightly enriched quantities of the elements Si, Al, Ti, K and P, compared to CFA. It is noteworthy that Ca and Na were not enriched in either the MF or NMF material. These elements also exhibited relatively low total recoveries after magnetic separation (Table S1, Supplementary Information), indicating that these minerals may have dissolved into aqueous solution during the magnetic separation process due to their high solubility. Similarly, the dissolution of soluble components in CFA such as Na,

K, Ca, Mg and SO<sub>4</sub> has been reported in the literature [60]. The wet magnetic separation process therefore served as a relatively easy technique to separate Fe-containing minerals from the other matrix elements in CFA (contained in silicate/aluminosilicate-containing minerals). The wet, magnetic separation process also aided in the dissolution of soluble Ca species into aqueous solution. Fe and Ca species may hinder the recovery and utilisation of silicates and other valuable minerals during further processing; this is particularly evident in the process of zeolitisation [61,62].

**Table 5.** Trace elemental composition of the fractions of CFA (NMF and MF) characterised by LA-ICP-MS spectroscopy (n = 3), as well as the enrichment factor (EF) of each component relative to CFA. \*: Rare earth element.

Trace Elements	Nonmagnetic Fraction			Magnetic Fraction		
	ppm	Relative Standard Deviation	EF	ppm	Relative Standard Deviation	EF
Ba	913.00	7.87	1.03	743.90	18.90	0.84
Sr	838.50	8.20	1.04	605.37	21.15	0.75
Zr	422.97	8.09	1.01	267.40	22.70	0.64
Ce *	188.13	1.23	1.08	116.57	6.23	0.67
V	119.07	1.64	0.95	126.10	3.31	1.00
La *	92.90	1.04	1.09	56.85	2.08	0.66
Ni	62.30	1.98	0.93	183.47	10.72	2.73
Y *	67.91	0.49	1.04	45.98	1.22	0.70
Nd *	70.67	1.02	1.08	44.70	2.22	0.69
Zn	59.20	0.88	1.17	79.70	4.75	1.57
Pb	50.00	1.41	1.26	26.49	2.27	0.67
Cu	47.97	4.06	1.26	58.83	16.01	1.54
Th	37.49	0.53	1.16	20.99	0.81	0.65
Nb	31.89	0.65	1.05	18.81	1.11	0.62
Rb	30.34	0.43	1.10	14.11	0.94	0.51
Sc *	30.77	0.16	1.17	22.16	0.93	0.84
Co	21.96	0.52	0.90	74.37	4.37	3.05
Pr *	19.48	0.10	1.06	12.10	0.63	0.66
Sm *	13.78	0.47	1.08	8.78	0.62	0.69
Gd *	12.48	0.52	1.10	8.29	0.51	0.73
Dy *	12.19	0.12	1.08	7.96	0.39	0.71
Hf	11.45	0.19	1.07	7.43	0.53	0.69
U	9.70	0.19	1.12	9.59	0.17	1.11
Er *	6.88	0.15	1.09	4.62	0.24	0.73
Yb *	6.26	0.11	1.09	4.37	0.35	0.76
Cs	5.84	0.06	1.19	2.40	0.25	0.49
Mo	4.28	0.28	0.94	8.19	0.39	1.80
Eu *	2.55	0.04	1.11	1.67	0.11	0.73
Ta	2.54	0.02	1.12	1.37	0.11	0.61
Ho *	2.42	0.04	1.10	1.57	0.12	0.71
Tb *	1.88	0.02	1.10	1.23	0.04	0.72
Tm *	0.95	0.01	1.09	0.63	0.02	0.73
Lu *	0.93	0.04	1.15	0.61	0.02	0.76

#### Enrichment of Trace Elements of CFA Components by Wet Magnetic Separation

The enrichment factors of trace elements in the MF and NMF material are listed in Table 5. Compared to CFA, the MF material contained enriched quantities of transition metals Ni, Zn, Cu, Co and Mo (EF values > 1) and retained the quantity of V (EF = 1). This may be due to the close association of these transition metal elements with Fe in mineral phases such as bornite (Cu), chalcopyrite (Cu), eskebornite (Cu), pentlandite (Ni) and staurolite (Zn), as reported by Finkelman et al. [50]. It is noteworthy that the MF material also contained a slightly enriched quantity of U (EF = 1.1). The majority of the other trace elements were enriched in the NMF material relative to the quantities present in CFA, although enrichment factors were minor (EF values = ~1.1–1.3). As expected,

reduced quantities of transition metal elements V, Ni, Co and Mo were observed in the NMF material (with EF values < 1), compared to CFA.

Overall, the wet magnetic separation process was able to partition a specific set of transition metal elements (Fe, Mn, Cr, V, Ni, Zn, Cu, Co and Mo present in various quantities) into the MF material, while partitioning the trace REEs into the NMF material. Furthermore, soluble species in CFA such as Ca and Na were removed from matrix minerals (silicates and aluminosilicates) through dissolution during the wet, magnetic separation process. The wet, magnetic separation process may therefore be considered as a pre-processing step for separating Fe-containing minerals (as well as soluble Ca and Na minerals) from the other matrix elements of CFA, which are known to exist in association with the majority of the REE content contained in CFA [9,42].

### 3.3. Zeolitisation

#### 3.3.1. Mineralogical Composition of the Zeolite Product and Si Extract

Liquid phase, alkaline treatment of the NMF was carried out at 150 °C and resulted in a solid zeolite product and filtrate solution. The Si extract was precipitated from the filtrate solution by addition of a mineral acid. The variation in the mineralogical content between the NMF, zeolite and Si extract were analysed by XRD (depicted in Figure 4). Most of the quartz and mullite mineral phases present in the NMF material were converted to a crystalline zeolite product (hydroxysodalite) during the liquid phase alkaline treatment process. Zeolitisation occurred via chemical processes of hydrolysis/depolymerisation and dissolution (Equations (3)–(6)), and subsequently, condensation/polymerisation (Equation (7)) of aluminosilicate species (T = Al or Si) to form a crystalline zeolite framework, as adapted from Feijen et al. [63]. It is noteworthy that no solid waste was produced during the zeolitisation process. The Si extract was composed of amorphous silica and a sodium sulphate ( $\text{Na}_2\text{SO}_4$ ) crystalline mineral phase called thenardite [64–66].

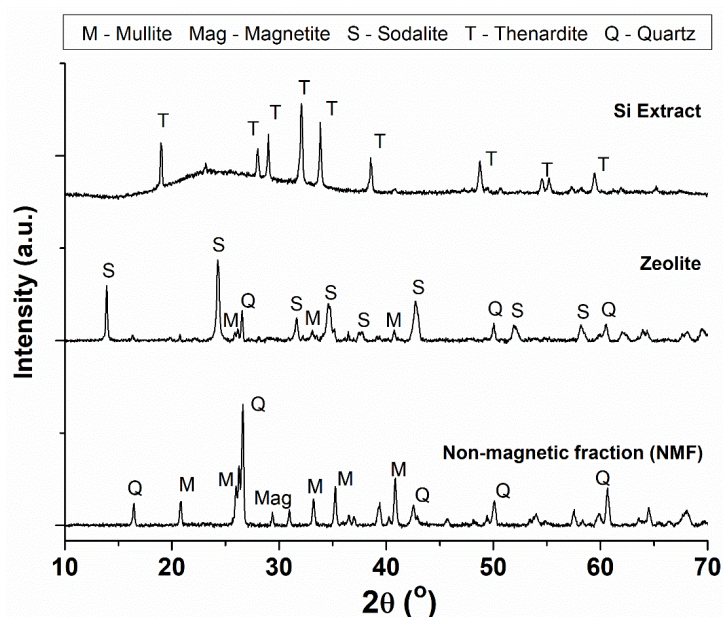
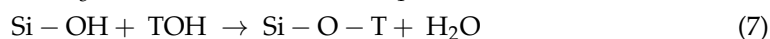
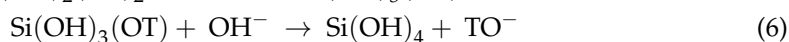
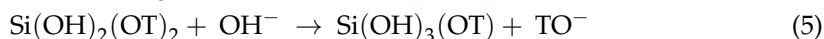
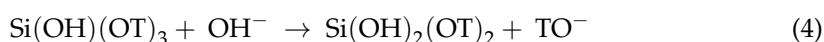
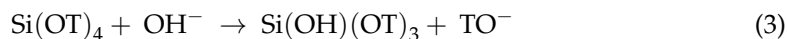


**Figure 4.** Powder XRD patterns of the NMF, zeolite and Si extraction generated by liquid phase alkaline treatment and precipitation.

### 3.3.2. Chemical Composition of the Zeolite and Si Extract

The chemical composition of the zeolite and Si extract was analysed by XRF (as listed in Table 6) and LA-ICP-MS (as listed in Table 7). The Si extract was made up of mainly Si and Na oxides (70.70 and 28.18 wt%, respectively) and contained a low quantity of Al and K oxides (0.49 and 0.45 wt%, respectively), as listed in Table 6. As expected, the zeolite was composed of mainly Si, Al and Na oxides (40.02, 26.83 and 22.56 wt%, respectively), and also contained a considerable amount of Ca (4.92 wt%). Additionally, major elements from the NMF material such as Ti, Mg, K, Mn and Cr were present in the zeolite product in minor quantities. On the other hand, these elements were present in very low quantities or quantities below the detection limits of the instrument in the Si extract.

**Table 6.** Major oxide composition (dry weight) of the zeolite and Si extract prepared using the NMF characterised by XRF spectroscopy (n = 3), as well as the enrichment factor (EF) of each component relative to CFA. L.O.I.: Loss on ignition; b.d.l.: below detection limits; -: not applicable.

Major Elements	Si Extract				Zeolite		
	wt%	Relative Standard Deviation	EF	wt%	Relative Standard Deviation	EF	
SiO <sub>2</sub>	70.70	2.50	1.25	40.02	0.97	0.71	
Al <sub>2</sub> O <sub>3</sub>	0.49	0.14	0.02	26.83	1.21	0.97	
Fe <sub>2</sub> O <sub>3</sub>	0.02	0.01	0.00	2.19	0.04	0.36	
CaO	0.05	0.02	0.01	4.92	0.03	0.88	
TiO <sub>2</sub>	0.07	0.02	0.04	1.50	0.06	0.94	
MgO	b.d.l	b.d.l	0.00	1.39	0.03	0.88	
K <sub>2</sub> O	0.45	0.11	0.79	0.39	0.07	0.68	
P <sub>2</sub> O <sub>5</sub>	0.03	0.01	0.08	0.13	0.00	0.36	
Na <sub>2</sub> O	28.18	1.56	301.72	22.56	1.27	241.55	
MnO	b.d.l	b.d.l	0.00	0.04	0.00	0.75	
Cr <sub>2</sub> O <sub>3</sub>	b.d.l	b.d.l	0.00	0.02	0.00	1.00	
Sum	100.00	-	-	100.00	-	-	
L.O.I	7.23	2.18	-	18.59	1.12	-	

The trace elemental content of the zeolite was relatively high compared to that of the Si extract, as listed in Table 7. In general, both the zeolite and Si extract material contained low levels of trace elements in comparison to the NMF material as well as CFA. A few exceptions occurred for the zeolite material, which included Hf, Zr and Ce (REE) that were present at relatively high levels in the zeolite material relative to CFA. This may be due to the incorporation of these elements into the zeolite framework as extra-framework species and/or the close association of these elements with CFA aluminosilicate mineral phases involved in the process of zeolitisation. Ce is known to be present in the coal-derived bastnasite and Al-containing mineral florencite [37,50,67]. In the case of the Si extract, trace elements such as Dy, Er, Eu, Gd, Nd, Sm, Tb, Tm and Yb were below the detection limits of the instrument, while other trace elements were present at very low levels (<100 ppm). This was likely due to the exclusion of these elements from the Si extract material during the process of precipitation. This phenomenon occurs during the crystallization of thenardite from the Si-rich filtrate solution whereby solvated silicate species are incorporated into the crystalline material that precipitates out of the solution, while other soluble impurities were excluded from the crystalline material or largely remained in solution [68,69].

#### Enrichment of Major Elements of CFA Components by Zeolitisation

During zeolitisation, the major elements partitioned into the liquid and solid phase based on the alkaline reflux conditions applied to the mixture. As listed in Table 6, the zeolite material (solid phase collected by filtration) exhibited less enriched levels of the major elements relative to CFA (EF < 1) with the exception of Cr that exhibited an EF = 1. High EF values were observed for Na due to the addition of NaOH during the zeolitisation process, i.e., EF = 242 and 302 for the zeolite product and Si extract, respectively. In the case of the Si extract (collected by precipitation from the liquid phase filtrate), the

partial enrichment of Si (EF = 1.25) was achieved. The other major elements were largely excluded from the Si extract, as indicated by the very low EFs (EF << 1) relative to CFA. It is noteworthy that the Si extract was nearly free of Al and Fe oxides and may therefore serve as a suitable Si feedstock in other Si-based applications.

**Table 7.** Trace elemental composition of the zeolite and Si extract prepared using the NMF by LA-ICP-MS spectroscopy (n = 3), as well as the enrichment factor (EF) of each component relative to CFA. \* Rare earth element; b.d.l: below detection limits.

Trace Elements	Si Extract			Zeolite		
	ppm	Relative Standard Deviation	EF	ppm	Relative Standard Deviation	EF
Ba	47.60	11.40	0.05	751.40	30.46	0.85
Sr	3.76	0.94	0.00	688.27	35.05	0.85
Zr	84.40	8.20	0.20	492.67	20.16	1.18
Ce *	0.57	0.02	0.00	259.13	18.13	1.49
V	28.55	6.95	0.16	28.01	1.56	0.16
La *	0.10	0.00	0.00	75.37	4.53	0.88
Ni	6.05	0.16	0.05	48.57	2.67	0.39
Y *	0.09	0.04	0.00	56.06	3.84	0.86
Nd *	0.00	0.00	0.00	57.73	3.37	0.89
Zn	57.65	33.35	0.88	30.33	3.52	0.46
Pb	38.20	0.20	0.75	20.73	6.82	0.41
Cu	10.48	1.53	0.26	41.16	4.96	1.03
Th	0.03	0.00	0.00	30.35	2.20	0.79
Nb	2.12	1.05	0.07	25.14	1.37	0.78
Rb	13.91	3.15	0.46	9.26	0.85	0.31
Sc *	3.48	0.13	0.12	23.93	1.03	0.87
Co	0.59	0.11	0.02	16.72	1.00	0.64
Pr *	0.01	0.00	0.00	15.89	0.97	0.65
Sm *	b.d.l	b.d.l	0.00	11.09	0.69	0.60
Gd *	b.d.l	b.d.l	0.00	10.09	0.58	0.79
Dy *	b.d.l	b.d.l	0.00	10.05	0.46	0.88
Hf	2.16	0.18	0.19	12.98	0.62	1.15
U	1.68	0.90	0.16	7.29	0.94	0.68
Er *	b.d.l	b.d.l	0.00	5.70	0.31	0.66
Yb *	b.d.l	b.d.l	0.00	5.38	0.41	0.85
Cs	2.01	0.59	0.35	1.33	0.36	0.23
Mo	1.09	0.35	0.22	0.96	0.13	0.19
Eu *	b.d.l	b.d.l	0.00	2.07	0.17	0.91
Ta	0.35	0.14	0.08	1.97	0.12	0.43
Ho *	0.01	0.00	0.00	1.88	0.18	0.82
Tb *	b.d.l	b.d.l	0.00	1.55	0.09	0.70
Tm *	b.d.l	b.d.l	0.00	0.83	0.05	0.49
Lu *	0.02	0.00	0.02	0.80	0.07	0.92

#### Enrichment of Trace Elements of CFA Components by Zeolitisation

The trace elements also partitioned between the solid and liquid phase during zeolitisation (as listed in Table 7). The solid zeolite product contained reduced levels of trace elements (EF < 1), with the exception of Zr, Hf and Ce which were enriched compared to CFA (EF values of 1.2, 1.2 and 1.5, respectively). Zr, Hf and Ce typically exist as tetra- and tri-valent cations, respectively. These trace elements may therefore occupy extra-framework cation sites in the centre of the 6-ring and  $\beta$ -cage (sodalite cage) of the sodalite crystal structure [70]. These results indicated that most of the trace elements were enriched into the liquid phase filtrate collected after zeolitisation. The precipitation of the Si extract from the filtrate resulted in a highly pure Si material with little to no trace elements present (i.e., EF values << 1). Therefore, the supernatant liquid collected after the precipitation of the Si extract from the filtrate is thought to be highly enriched with trace elements, compared to CFA.

### 3.4. The Partitioning of REEs from CFA by Wet, Magnetic Separation Coupled to Zeolitisation

The partitioning of REEs from CFA into the products of wet, magnetic separation and zeolitisation (as well as Si extraction through precipitation) is depicted in Figure 5. During the wet, magnetic separation process REEs were all enriched into the NMF material with a total REE content of 530.2 ppm, which is ~3 times more enriched compared to the earth's upper crust [4]. REEs are proposed to be closely associated with mineral phases quartz and/or mullite in the NMF material. It was previously reported that REEs are present in the glassy aluminosilicate particles in CFA [11,38]. During the zeolitisation process, Ce was selectively partitioned into the zeolite product, while the other REEs were partitioned into the filtrate solution. This is in contrast to the study by Du Plessis et al. [26], where nonselective Ce enrichment into the bulk solid product/waste was reported together with REE Y, while the other REEs were not monitored. The precipitation of the Si extract from the filtrate solution resulted in a solid precipitation product that was nearly free of REEs, which indicated that other REEs were partitioned into the supernatant solution collected after Si precipitation.

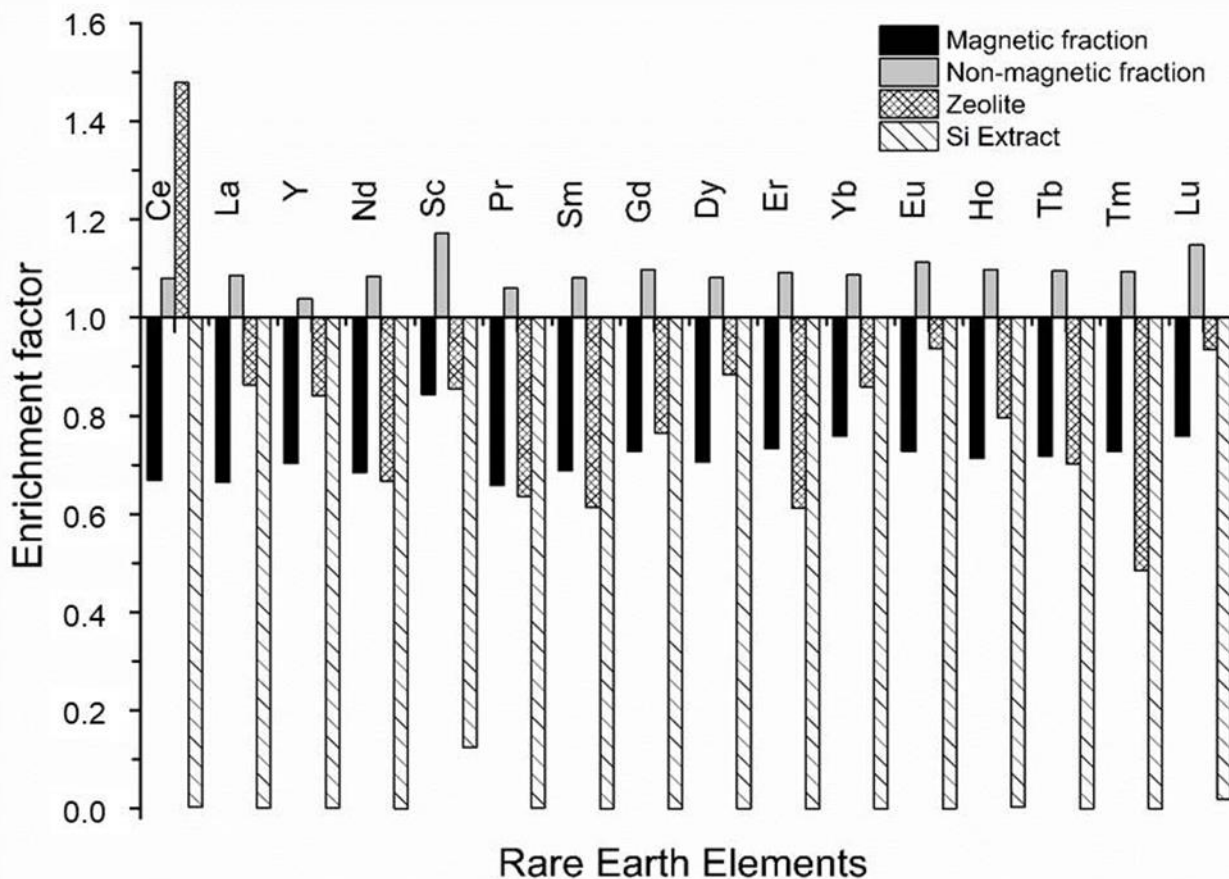


**Figure 5.** Enrichment factors for REEs in CFA during the processes of magnetic separation and zeolitisation (baseline EF = 1).

This provides an opportunity for REE recovery from the solid zeolite or aqueous supernatant solution by application of methods such as ion-exchange, leaching, membrane separation/nanofiltration and/or functionalised ligands [6,9,71–76]. Zeolites are known for their ion-exchange properties and this property may be exploited to recover Ce from the crystallite hydroxysodalite framework via ion-exchange with a salt solution [71,72,76]. Similarly, Ce may be leached from the hydroxysodalite framework and recovered by nanofiltration [6,9,73]. Perea et al. [74] recently reported the recovery of Ce and Nd from aqueous solutions using diglycolic acid functionalised electrospun polystyrene nanofibers as a ligand. This approach may also be applied for the recovery of REEs from aqueous supernatant solution and/or leachate from the crystalline zeolite product.

It is noteworthy that the zeolite product contained a similar total REE content (537.6 ppm) to the NMF material (530.2 ppm). Therefore, both the zeolite product and NMF material contained total REE levels ~3 times that of the earth's crust [4]. Although the total REE content in these products are similar to that of CFA, the processing of CFA by wet, magnetic separation and subsequent zeolitisation of the NMF allowed for the selective partitioning of a particular REE (Ce) into the solid zeolite product (hydroxysodalite), while other REEs were largely dissolved into the aqueous supernatant solution. Therefore, this study illustrated that a simple process utilised for the recovery of Fe and Si from CFA together with the production of an industrially valuable material (i.e., a crystalline zeolite), also has the potential for REE recovery from the aqueous supernatant solution and/or zeolite product. This is in contrast to the utilisation of ionic liquids in a complex multi-stage process for the separation of the matrix elements of CFA from REEs [6]. Furthermore, the Ce selectivity of hydroxysodalite may be as a result of the geometric and electronic structure of the sodalite cages that make up this zeolite framework. It may be of interest to evaluate the REE selectivity other zeolites typically synthesised from CFA in the future as well as compare this method of CFA zeolitisation with other protocols in terms of REE recovery and enrichment.

#### 4. Conclusions

South African CFA was processed by wet, magnetic separation and subsequent zeolitisation of the NMF by liquid alkaline treatment. The wet, magnetic separation process removed the majority of iron-containing mineral phases from the bulk of CFA, yielding the MF material (8.4 wt%) and NMF material (91.6 wt%). During the wet, magnetic separation process, it was found that all REEs present in CFA partitioned into the NMF, while transition metal elements (such as Mn, Cr, V, Ni, Zn, Cu, Co and Mo) were partitioned into the MF along with Fe. Zeolitisation of the NMF resulted in the selective partitioning of Ce into the solid zeolite hydroxysodalite, while other REEs largely partitioned into the liquid phase.

The total REE content of the NMF was enriched (530.2 ppm) compared to natural resources found in the earth's upper crust, which are typically utilised for REE recovery and production worldwide. Similarly, the total REE content of the zeolite product was enriched (537.6 ppm) with Ce (259.1 ppm) compared to CFA, as well as other sources of Ce such as WEEEs. This study therefore highlights the potential for CFA to serve as a viable alternative resource for REEs through simple processing steps such as wet, magnetic separation and particularly zeolitisation to selectively recover REEs while extracting other industrially valuable products such as Fe and Si (and Al) from CFA. More importantly, this study demonstrates that countries which produce large quantities of CFA as a waste by-product of coal combustion may develop this processing technology for the recovery of REEs from alternative resources, as well as for the production of REEs for the global market.

**Supplementary Materials:** The following are available online at <https://www.mdpi.com/article/10.3390/min11090950/s1>, Figure S1: SEM micrographs of as-received CFA, magnetic fraction and nonmagnetic fraction generated by wet magnetic separation. Figure S2: SEM micrographs of the nonmagnetic fraction of CFA as well as the zeolite product and Si extract generated by liquid phase alkaline treatment and precipitation. Table S1: Recovery of main components of CFA in magnetic separation products (nonmagnetic and magnetic fraction).

**Author Contributions:** Conceptualization, M.-L.U.C. and L.F.P.; methodology, M.-L.U.C.; validation, M.-L.U.C.; formal analysis, M.-L.U.C.; investigation, M.-L.U.C. and A.E.A.; resources, L.F.P.; writing—original draft preparation, M.-L.U.C.; writing—review and editing, M.-L.U.C., A.E.A., C.P.E., O.F., A.S. and L.F.P.; visualization, M.-L.U.C.; supervision, L.F.P. and A.S.; project administration, M.-L.U.C.; funding acquisition, L.F.P. All authors have read and agreed to the published version of the manuscript.

**Funding:** The authors would like to thank the National Research Foundation (NRF) of South Africa for funding the research project and the Commonwealth Scholarship Commission in the United

Kingdom for funding the research visit to the University of Bath, United Kingdom. Asel Sartbaeva would further like to thank the Royal Society and British Council for funding.

**Data Availability Statement:** Data is contained within the article or Supplementary Material.

**Acknowledgments:** The authors would like to thank the CAF Analytical facilities at Stellenbosch University for their assistance. Furthermore, the authors would like to express their appreciation for the academic support of the Environmental and Nano Sciences (ENS) research group at the University of the Western Cape (South Africa) and the Sartbaeva research group at the University of Bath (United Kingdom) during the research project.

**Conflicts of Interest:** The authors declare no conflict of interest.

## References

- Zhou, B.; Li, Z.; Chen, C. Global Potential of Rare Earth Resources and Rare Earth Demand from Clean Technologies. *Minerals* **2017**, *7*, 203. [\[CrossRef\]](#)
- Charalampides, G.; Vatalis, K.I.; Apostoplos, B.; Ploutarch-Nikolas, B. Rare Earth Elements: Industrial Applications and Economic Dependency of Europe. *Procedia Econ. Financ.* **2015**, *24*, 126–135. [\[CrossRef\]](#)
- Gao, S. *Chemical Composition of the Continental Crust: A Perspective from China*; Geochemical Society: Washington, DC, USA, 2010; Volume 143, p. 16.
- Rudnick, R.L.; Gao, S. Composition of the continental crust. *Treatise Geochem.* **2003**, *3*, 1–64.
- McLeod, C.L.; Shaulis, B.J. Rare Earth Elements in Planetary Crusts: Insights from Chemically Evolved Igneous Suites on Earth and the Moon. *Minerals* **2018**, *8*, 455. [\[CrossRef\]](#)
- Rybak, A.; Rybak, A. Characteristics of Some Selected Methods of Rare Earth Elements Recovery from Coal Fly Ashes. *Metals* **2021**, *11*, 142. [\[CrossRef\]](#)
- Kumari, A.; Panda, R.; Jha, M.K.; Kumar, J.R.; Lee, J.-Y. Process development to recover rare earth metals from monazite mineral: A review. *Miner. Eng.* **2015**, *79*, 102–115. [\[CrossRef\]](#)
- Sahoo, P.K.; Kim, K.; Powell, M.A.; Equeenuddin, S.M. Recovery of metals and other beneficial products from coal fly ash: A sustainable approach for fly ash management. *Int. J. Coal Sci. Technol.* **2016**, *3*, 267–283. [\[CrossRef\]](#)
- Zhang, W.; Honaker, R. Enhanced leachability of rare earth elements from calcined products of bituminous coals. *Miner. Eng.* **2019**, *142*, 105935. [\[CrossRef\]](#)
- Crowley, S.S.; Stanton, R.W.; Ryer, T.A. The effects of volcanic ash on the maceral and chemical composition of the C coal bed, Emery Coal Field, Utah. *Org. Geochem.* **1989**, *14*, 315–331. [\[CrossRef\]](#)
- Franus, W.; Wiatros-Motyka, M.M.; Wdowin, M. Coal fly ash as a resource for rare earth elements. *Environ. Sci. Pollut. Res.* **2015**, *22*, 9464–9474. [\[CrossRef\]](#)
- Hower, J.C.; Eble, C.F.; Dai, S.; Belkin, H.E. Distribution of rare earth elements in eastern Kentucky coals: Indicators of multiple modes of enrichment? *Int. J. Coal Geol.* **2016**, *160–161*, 73–81. [\[CrossRef\]](#)
- Seredin, V.V.; Dai, S. Coal deposits as potential alternative sources for lanthanides and yttrium. *Int. J. Coal Geol.* **2012**, *94*, 67–93. [\[CrossRef\]](#)
- Lin, R.; Howard, B.H.; Roth, E.; Bank, T.L.; Granite, E.J.; Soong, Y. Enrichment of rare earth elements from coal and coal by-products by physical separations. *Fuel* **2017**, *200*, 506–520. [\[CrossRef\]](#)
- Nyale, S.M.; Babajide, O.O.; Birch, G.D.; Böke, N.; Petrik, L.F. Synthesis and Characterization of Coal Fly Ash-based Foamed Geopolymer. *Procedia Environ. Sci.* **2013**, *18*, 722–730. [\[CrossRef\]](#)
- Blissett, R.; Rowson, N. A review of the multi-component utilisation of coal fly ash. *Fuel* **2012**, *97*, 1–23. [\[CrossRef\]](#)
- Eze, C.P.; Fatoba, O.; Madzivire, G.; Ostrovnyaya, T.M.; Petrik, L.F.; Frontasyeva, M.V.; Nechaev, A.N. Elemental composition of fly ash: A comparative study using nuclear and related analytical techniques. *Chem. Didact. Ecol. Metrol.* **2013**, *18*, 19–29. [\[CrossRef\]](#)
- Huang, Z.; Fan, M.; Tiand, H. Coal and coal byproducts: A large and developable unconventional resource for critical materials—Rare earth elements. *J. Rare Earths* **2018**, *36*, 337–338. [\[CrossRef\]](#)
- Chindapasirt, P.; Boonbamrung, T.; Poolsong, A.; Kroehong, W. Effect of elevated temperature on polypropylene fiber reinforced alkali-activated high calcium fly ash paste. *Case Stud. Constr. Mater.* **2021**, *15*, e00554. [\[CrossRef\]](#)
- Mastali, M.; Abdollahnejad, Z.; Pacheco-Torgal, F. 16—Carbon dioxide sequestration of fly ash alkaline-based mortars containing recycled aggregates and reinforced by hemp fibers: Properties, freeze-thaw resistance, and carbon footprint. In *Woodhead Publishing Series in Civil and Structural Engineering, Carbon Dioxide Sequestration in Cementitious Construction Materials*; Pacheco-Torgal, F., Caijun, S., Sanchez, A.P., Eds.; Woodhead Publishing: Cambridge, UK, 2018; pp. 393–409.
- Roopchund, R.; Andrew, J.; Sithole, B. Using cellulose nanocrystals to improve the mechanical properties of fly ash-based geopolymer construction materials. *Eng. Sci. Technol. Int. J.* **2021**, in press. [\[CrossRef\]](#)
- Top, S.; Vapur, H.; Altiner, M.; Kaya, D.; Ekicibil, A. Properties of fly ash-based lightweight geopolymer concrete prepared using pumice and expanded perlite as aggregates. *J. Mol. Struct.* **2020**, *1202*, 127236. [\[CrossRef\]](#)
- Wang, L.; Huang, X.; Zhang, J.; Wu, F.; Liu, F.; Zhao, H.; Hu, X.; Zhao, X.; Li, J.; Ju, X.; et al. Stabilization of lead in waste water and farmland soil using modified coal fly ash. *J. Clean. Prod.* **2021**, *314*, 127957. [\[CrossRef\]](#)



24. Ameh, A.E.; Eze, C.P.; Antunes, E.; Cornelius, M.-L.U.; Musyoka, N.; Petrik, L.F. Stability of fly ash-based BEA-zeolite in hot liquid phase. *Catal. Today* **2020**, *357*, 416–424. [[CrossRef](#)]
25. Ameh, A.E.; Musyoka, N.M.; Fatoba, O.O.; Syrtsova, D.A.; Teplyakov, V.V.; Petrik, L.F. Synthesis of zeolite NaA membrane from fused fly ash extract. *J. Environ. Sci. Health Part A* **2016**, *51*, 348–356. [[CrossRef](#)]
26. Du Plessis, P.W.; Ojumu, T.V.; Fatoba, O.O.; Akinyeye, R.O.; Petrik, L.F. Distributional Fate of Elements during the Synthesis of Zeolites from South African Coal Fly Ash. *Materials* **2014**, *7*, 3305–3318. [[CrossRef](#)]
27. Gilbert, C.; Ayanda, O.S.; Fatoba, O.O.; Madzivire, G.; Petrik, L.F. A Novel Method of Using Iron Nanoparticles from Coal Fly Ash or Ferric Chloride for Acid Mine Drainage Remediation. *Mine Water Environ.* **2019**, *38*, 617–631. [[CrossRef](#)]
28. Missengue, R.N.M.; Losch, P.; Musyoka, N.M.; Louis, B.; Pale, P.; Petrik, L.F. Conversion of South African Coal Fly Ash into High-Purity ZSM-5 Zeolite without Additional Source of Silica or Alumina and Its Application as a Methanol-to-Olefins Catalyst. *Catalysts* **2018**, *8*, 124. [[CrossRef](#)]
29. Missengue, R.N.M. Synthesis of ZSM-5 Zeolite from South African Fly Ash and Its Application as Solid Catalyst 2016. Ph.D. Thesis, University of the Western Cape, Cape Town, South Africa, 2016. Available online: <http://etd.uwc.ac.za/xmlui/handle/11394/5431> (accessed on 28 June 2019).
30. Missengue, R.; Losch, P.; Sedres, G.; Musyoka, N.; Fatoba, O.O.; Louis, B.; Pale, P.; Petrik, L.F. Transformation of South African coal fly ash into ZSM-5 zeolite and its application as an MTO catalyst. *C. R. Chim.* **2017**, *20*, 78–86. [[CrossRef](#)]
31. Mukaba, M.J.-L.; Ameh, A.E.; Eze, C.P.; Petrik, L.F. Evaluation of modified fly ash based naa-zeolite: Effect of crystallinity on CO<sub>2</sub> adsorption capacity. *Environ. Eng. Manag. J.* **2019**, *19*, 475–483. [[CrossRef](#)]
32. Musyoka, N.; Petrik, L.F.; Fatoba, O.O.; Hums, E. Synthesis of zeolites from coal fly ash using mine waters. *Miner. Eng.* **2013**, *53*, 9–15. [[CrossRef](#)]
33. Musyoka, N.M.; Petrik, L.F.; Hums, E.; Baser, H.; Schwieger, W. In situ ultrasonic diagnostic of zeolite X crystallization with novel (hierarchical) morphology from coal fly ash. *Ultrasonics* **2014**, *54*, 537–543. [[CrossRef](#)]
34. Ndlovu, N.Z.N.; Missengue, R.N.M.; Petrik, L.F.; Ojumu, T. Synthesis and Characterization of Faujasite Zeolite and Geopolymer from South African Coal Fly Ash. *J. Environ. Eng.* **2017**, *143*, 04017042. [[CrossRef](#)]
35. Van Der Merwe, E.M.; Gray, C.L.; Castleman, B.A.; Mohamed, S.; Kruger, R.A.; Doucet, F.J. Ammonium sulphate and/or ammonium bisulphate as extracting agents for the recovery of aluminium from ultrafine coal fly ash. *Hydrometallurgy* **2017**, *171*, 185–190. [[CrossRef](#)]
36. Blissett, R.; Smalley, N.; Rowson, N. An investigation into six coal fly ashes from the United Kingdom and Poland to evaluate rare earth element content. *Fuel* **2014**, *119*, 236–239. [[CrossRef](#)]
37. Zhang, W.; Rezaee, M.; Bhagavatula, A.; Li, Y.; Groppo, J.; Honaker, R. A Review of the Occurrence and Promising Recovery Methods of Rare Earth Elements from Coal and Coal By-Products. *Int. J. Coal Prep. Util.* **2015**, *35*, 295–330. [[CrossRef](#)]
38. Nugroho, N.D.; Rosita, W.; Perdana, I.; Bendiyasa, I.M.; Mufakhir, F.R.; Astuti, W. Iron bearing oxide minerals separation from rare earth elements (REE) rich coal fly ash. *IOP Conf. Ser. Mater. Sci. Eng.* **2019**, *478*, 012026. [[CrossRef](#)]
39. Valeev, D.; Kunilova, I.; Alpatov, A.; Varnavskaya, A.; Ju, D. Magnetite and Carbon Extraction from Coal Fly Ash Using Magnetic Separation and Flotation Methods. *Minerals* **2019**, *9*, 320. [[CrossRef](#)]
40. Lanzerstorfer, C. Pre-processing of coal combustion fly ash by classification for enrichment of rare earth elements. *Energy Rep.* **2018**, *4*, 660–663. [[CrossRef](#)]
41. Zhang, W.; Groppo, J.; Honaker, R. Ash Beneficiation for REE Recovery. In Proceedings of the World of Coal Ash Conference, Nashville, TN, USA, 5–7 May 2015.
42. Lin, R.; Stuckman, M.; Howard, B.H.; Bank, T.L.; Roth, E.A.; Macala, M.K.; Lopano, C.; Soong, Y.; Granite, E.J. Application of sequential extraction and hydrothermal treatment for characterization and enrichment of rare earth elements from coal fly ash. *Fuel* **2018**, *232*, 124–133. [[CrossRef](#)]
43. Sedres, G. Recovery of SiO<sub>2</sub> and Al<sub>2</sub>O<sub>3</sub> from Coal Fly Ash 2016. Master's Thesis, University of the Western Cape, Cape Town, South Africa, 2016. Available online: <http://etd.uwc.ac.za/handle/11394/5651> (accessed on 28 June 2019).
44. Ojha, K.; Pradhan, N.C.; Samanta, A.N. Zeolite from fly ash: Synthesis and characterization. *Bull. Mater. Sci.* **2004**, *27*, 555–564. [[CrossRef](#)]
45. Wdowin, M.; Franus, M.; Panek, R.; Badura, L.; Franus, W. The conversion technology of fly ash into zeolites. *Clean Technol. Environ. Policy* **2014**, *16*, 1217–1223. [[CrossRef](#)]
46. Ahmadzadeh, M.; Romero, C.; McCloy, J. Magnetic analysis of commercial hematite, magnetite, and their mixtures. *AIP Adv.* **2018**, *8*, 056807. [[CrossRef](#)]
47. Stracher, G.B.; Prakash, A.; Sokol, E.V. Mineralogy and Magnetic Parameters of Materials Resulting from the Mining and Consumption of Coal from the Douro Coalfield, Northwest Portugal. In *Coal and Peat Fires: A Global Perspective*; Elsevier: Amsterdam, The Netherlands, 2015; Volume 3, pp. 493–508.
48. Franus, W. Characterization of X-type zeolite prepared from coal fly ash. *Pol. J. Environ. Stud.* **2012**, *21*, 337–343.
49. Lian, S.; Wang, E.; Kang, Z.; Bai, Y.; Gao, L.; Jiang, M.; Hu, C.; Xu, L. Synthesis of magnetite nanorods and porous hematite nanorods. *Solid State Commun.* **2004**, *129*, 485–490. [[CrossRef](#)]
50. Finkelman, R.B.; Dai, S.; French, D. The importance of minerals in coal as the hosts of chemical elements: A review. *Int. J. Coal Geol.* **2019**, *212*, 103251. [[CrossRef](#)]

51. Ibrahim, L. Chemical characterization and mobility of metal species in fly ash–water system. *Water Sci.* **2015**, *29*, 109–122. [CrossRef]
52. Shaheen, S.M.; Hooda, P.S.; Tsadilas, C.D. Opportunities and challenges in the use of coal fly ash for soil improvements—A review. *J. Environ. Manag.* **2014**, *145*, 249–267. [CrossRef]
53. Haque, N.; Hughes, A.; Lim, S.; Vernon, C. Rare Earth Elements: Overview of Mining, Mineralogy, Uses, Sustainability and Environmental Impact. *Resources* **2014**, *3*, 614–635. [CrossRef]
54. Li, K.; Chen, J.; Zou, D. Extraction and Recovery of Cerium from Rare Earth Ore by Solvent Extraction. *Cerium Oxide Appl. Attrib.* **2019**. [CrossRef]
55. Binnemans, K.; Jones, P.T.; Blanpain, B.; Van Gerven, T.; Yang, Y.; Walton, A.; Buchert, M. Recycling of rare earths: A critical review. *J. Clean. Prod.* **2013**, *51*, 1–22. [CrossRef]
56. Cesaro, A.; Marra, A.; Kuchta, A.; Belgiorno, V.; van Hullebusch, E.D. WEEE management in a circular economy perspective: An overview. *Glob. NEST J.* **2018**, *20*, 743–750. [CrossRef]
57. Jowitt, S.M.; Werner, T.T.; Weng, Z.; Mudd, G.M. Recycling of the rare earth elements. *Curr. Opin. Green Sustain. Chem.* **2018**, *13*, 1–7. [CrossRef]
58. Valeev, D.; Mikhailova, A.; Atmadzhidi, A. Kinetics of Iron Extraction from Coal Fly Ash by Hydrochloric Acid Leaching. *Metals* **2018**, *8*, 533. [CrossRef]
59. Fatoba, O.O. Chemical Interactions and Mobility of Species in Fly Ash-Brine Co-Disposal Systems 2010. Ph.D. Thesis, University of the Western Cape, Cape Town, South Africa, 2010.
60. Gitari, W.M.; Fatoba, O.O.; Petrik, L.F.; Vadapalli, V.R. Leaching characteristics of selected South African fly ashes: Effect of pH on the release of major and trace species. *J. Environ. Sci. Health Part A* **2009**, *44*, 206–220. [CrossRef]
61. Valdés, M.G.; Pérez-Cordoves, A.; Díaz-García, M. Zeolites and zeolite-based materials in analytical chemistry. *TrAC Trends Anal. Chem.* **2006**, *25*, 24–30. [CrossRef]
62. Yu, J. Chapter 3—Synthesis of Zeolites. In *Studies in Surface Science and Catalysis*; Čejka, J., van Bekkum, H., Corma, A., Schüth, F., Eds.; Elsevier: Amsterdam, The Netherlands, 2007; Volume 168, pp. 39–103.
63. Feijen, E.J.; Martens, J.A.; Jacobs, P.A.; Weitkamp, J.; Karge, H.G.; Pfeifer, H.; Hölderich, W. Zeolites and their Mechanism of Synthesis. *Adv. Pharmacol.* **1994**, *84*, 3–21. [CrossRef]
64. Bricni, A.; Hammi, H.; Aggoun, S.; Mnif, A. Optimisation of magnesium oxychloride cement properties by silica glass. *Adv. Cem. Res.* **2016**, *28*, 654–663. [CrossRef]
65. Lafuente, B.; Downs, R.T.; Yang, H.; Stone, N. Chapter 1—The power of databases: The RRUFF project. In *Highlights Mineralogical Crystallography*; Armbruster, T., Danisi, R.M., Eds.; De Gruyter: Berlin, Germany, 2015; pp. 1–30.
66. Treacy MM, J.; Higgins, J.B. *Collection of Simulated XRD Powder Patterns for Zeolites*, 5th ed.; Elsevier: Amsterdam, The Netherlands, 2007; Available online: <https://www.elsevier.com/books/collection-of-simulated-xrd-powder-patterns-for-zeolites-fifth-5th-revised-edition/treacy/978-0-444-53067-7> (accessed on 28 June 2019).
67. Dai, S.; Finkelman, R.B. Coal as a promising source of critical elements: Progress and future prospects. *Int. J. Coal Geol.* **2018**, *186*, 155–164. [CrossRef]
68. Richards, T.W. The inclusion and occlusion of solvent in crystals. An insidious source of error in quantitative chemical investigation. *Proc. Am. Philos. Soc.* **1903**, *42*, 28–36. Available online: <https://www.jstor.org/stable/983640> (accessed on 31 July 2021).
69. Urwin, S.J.; Levilain, G.; Marziano, I.; Merritt, J.M.; Houson, I.; Ter Horst, J.H. A Structured Approach to Cope with Impurities during Industrial Crystallization Development. *Org. Process. Res. Dev.* **2020**, *24*, 1443–1456. [CrossRef]
70. Baerlocher, C.; McCusker, L.B. Database of Zeolite Structures 2017. Available online: <http://www.iza-structure.org/databases/> (accessed on 1 October 2018).
71. Chang, H.-L.; Shih, W.-H. A General Method for the Conversion of Fly Ash into Zeolites as Ion Exchangers for Cesium. *Ind. Eng. Chem. Res.* **1998**, *37*, 71–78. [CrossRef]
72. Chang, H.-L.; Shih, W.-H. Synthesis of Zeolites A and X from Fly Ashes and Their Ion-Exchange Behavior with Cobalt Ions. *Ind. Eng. Chem. Res.* **2000**, *39*, 4185–4191. [CrossRef]
73. Pan, J.; Hassas, B.V.; Rezaee, M.; Zhou, C.; Pisupati, S.V. Recovery of rare earth elements from coal fly ash through sequential chemical roasting, water leaching, and acid leaching processes. *J. Clean. Prod.* **2021**, *284*, 124725. [CrossRef]
74. Pereao, O.; Laatikainen, K.; Bode-Aluko, C.A.; Kochnev, I.; Fatoba, O.; Nechaev, A.; Petrik, L. Adsorption of Ce<sup>3+</sup> and Nd<sup>3+</sup> by diglycolic acid functionalised electrospun polystyrene nanofiber from aqueous solution. *Sep. Purif. Technol.* **2020**, *233*, 116059. [CrossRef]
75. Pereao, O.; Laatikainen, K.; Bode-Aluko, C.; Fatoba, O.; Omoniyi, E.; Kochnev, Y.; Nechaev, A.; Apel, P.; Petrik, L. Synthesis and characterisation of diglycolic acid functionalised polyethylene terephthalate nanofibers for rare earth elements recovery. *J. Environ. Chem. Eng.* **2021**, *9*, 105902. [CrossRef]
76. Xie, J.; Huang, M.; Kaliaguine, S. Base and acid sites in alkaline earth cation-exchanged X zeolites. *Catal. Lett.* **1994**, *29*, 281–291. [CrossRef]